MOEM

Modern Electronic Materials 2023; 9(2): 39–44
DOI 10.3897/j.moem.9.2.108161

Research Article

Crystal structure, piezoelectric and magnetic properties of $BiMn_{1-x}Fe_xO_3$ ($x \le 0.4$) solid solutions

Maxim V. Silibin[1], Dmitry A. Kiselev[2], Sergey I. Latushko[1,3], Dmitry V. Zheludkevich[1,3], Polina A. Sklyar[2], Dmitry V. Karpinsky[1,3]

1 National Research University "Moscow Institute of Electronic Technology", 1 Shokin Sq., Zelenograd, Moscow 124498, Russian Federation

2 National University of Science and Technology "MISIS", 4-1 Leninsky Ave., Moscow 119049, Russian Federation

3 Scientific-Practical Materials Research Centre of the National Academy of Sciences of Belarus, 19 P. Brovka Str., Minsk 220072, Republic of Belarus

Corresponding author: Dmitry V. Karpinsky (dmitry.karpinsky@gmail.com)

Received 13 April 2023 ♦ **Accepted** 19 June 2023 ♦ **Published** 3 July 2023

Citation: Silibin MV, Kiselev DA, Latushko SI, Zheludkevich DV, Sklyar PA, Karpinsky DV (2023) Crystal structure, piezoelectric and magnetic properties of $BiMn_{1-x}Fe_xO_3$ ($x \le 0.4$) solid solutions. *Modern Electronic Materials* 9(2): 39–44. https://doi.org/10.3897/j.moem.9.2.108161

Abstract

The crystal structure, piezoelectric and magnetic properties of $BiMn_{1-x}Fe_xO_3$ ($x \le 0.4$) solid solutions synthesized using different solid state reactions from a stoichiometric mixture of simple oxides at high pressures and temperatures have been studied. The structure of the composition undergoes a concentration phase transition from the monoclinic to the orthorhombic structure. The formation of the orthorhombic phase is observed at the concentration $x \approx 0.2$ and is accompanied by the destruction of the d_{z2} orbitals of the Mn^{3+} ions causing the stabilization of a homogeneous magnetic state. The solid solutions containing $0.2 \le x \le 0.4$ exhibit a non-zero piezoresponse and may have ferroelectric or magnetic domain structures, the ferroelectric switching voltage decreasing with an increase in the iron concentration while the remanent magnetization decreases. The highest piezoresponse signal is observed for the $BiMn_{0.7}Fe_{0.3}O_3$ solid solution. The relationship between the chemical composition, type of crystal structure, piezoelectric and magnetic properties of the $BiMn_{1-x}Fe_xO_3$ solid solutions has been verified. Due to the combination of magnetic and electric dipole ordering these materials show good promise for practical applications.

Keywords

crystal structure, phase composition, magnetic structure orbital ordering, ferroelectric domain structure, hysteresis

1. Introduction

The interest to multiferroics, i.e., materials combining two or more types of ferro-ordering such as ferromagnetism, ferroelectric effect and ferroelectric elasticity has grown up in recent years [1]. This is first of all caused by the discovery of new materials of this type possessing a wide application domain [2, 3]. For example, these materials can be used for the fabrication of magnetic memery components, new four-state logic devices, magnetoelectric gages etc.

Currently, $BiMnO_3$ and $BiFeO_3$ based materials are among the most widely used multiferroics [4–7]. $BiMnO_3$ and $BiFeO_3$ with Bi^{3+} ions pertain to the group of oxide Perovskites having the structural formula $BiXO_3$, where X is the trivalent transition metal. The research interest to $BiFeO_3$ is accounted for by the high

phase transition temperatures (the antiferromagnetic transition point $T_{Néel}$ = 643 K [8], the ferroelectric transition point T_{Curie} = 1103 K [7]) providing for possibility of using bismuth ferrite based materials at room temperature [9]. There are scarce literary data on the structure and properties of the $BiMn_{1-x}Fe_xO_3$ solid solutions because of the complexity of their synthesis [10–12]. The $(1-x)BiFeO_3$–$(x)BiMnO_3$ solid solutions with $0.2 < x < 0.8$ are known to undergo an irreversible change in the magnetic properties after magnetization at temperatures above the magnetic transition point [13] which also raises interest to these materials. For example, heating to ~773 K changes the structural state of the solid solutions which are two-phase in the initial state (at room temperature), suggesting a metastable nature of the crystal and magnetic structures of these solid solutions. In this work we present experimental results on the crystal structure, ferroelectric and magnetic properties of the $BiMn_{1-x}Fe_xO_3$ solid solutions with $x \leq 0.4$ depending on their chemical composition.

2. Experimental

The ceramic $BiMn_{1-x}Fe_xO_3$ solid solutions with x = 0, 0.2, 0.3 and 0.4 were synthesized using high-temperature solid state reactions from simple oxides Bi_2O_3, Fe_2O_3 and MnO_2 taken in the stoichiometric ratio. The synthesis was carried out in a high-pressure reactor at 6 GPa and ~1600 K for 40 min in soldered platinum ampoules. After the synthesis the pressure was gradually reduced to atmospheric one and the specimens were quenched at room temperature. The crystal and magnetic structure of the compositions was analyzed using X-ray diffraction on a PANalytical X'pert Pro diffractometer in CuK_α radiation (λ = 0.15406 nm). The X-ray data were analyzed using the Rietveld method with the FullProf software. The magnetization was measured with a CFMS Cryogenic ltd. Universal installation. The domain structure was visualized and the repolarization processes were studied using a Ntegra Prima nanolaboratiory (NT-MDT SI, Russia) in piezoresponse force microscopy mode (PFM) [14]. The vertical component of the PFM signal was recorded by applying 5 V 27 kHz AC voltage to a NSG10/TiN (Tipsnano) conducting probe. The surface potential distribution was mapped in the Kelvin mode. The residual piezoelectric hysteresis loops were recorded with an MFP-3D™ StandAlone multifunctional scanning probe microscope (Oxford Instruments Asylum Research, USA) in DART mode near the cantilever/specimen contact resonance (~1.1 MHz) [15]. Magnetic force microscopy (MFM) measurements and phase composition studies were carried out using an MFM-LM (Tipsnano) cantilever coated with CoCr.

3. Results and discussion

3.1. Crystal structure of $BiMn_{1-x}Fe_xO_3$ solid solutions

Analysis of the X-ray diffraction patterns showed that an increase in the iron concentration to 20 mol.% leads to a structural phase transition from the monoclinic phase ($C2/c$ space group) to the orthorhombic phase (*Pnma* space group) described by the $\sqrt{2}a_p \cdot 4a_p \cdot 2\sqrt{2}a_p$ metric, where a_p is the Perovskite unit cell parameter. Figure 1 shows the diffraction pattern of the $BiMn_{0.7}Fe_{0.3}O_3$ solid

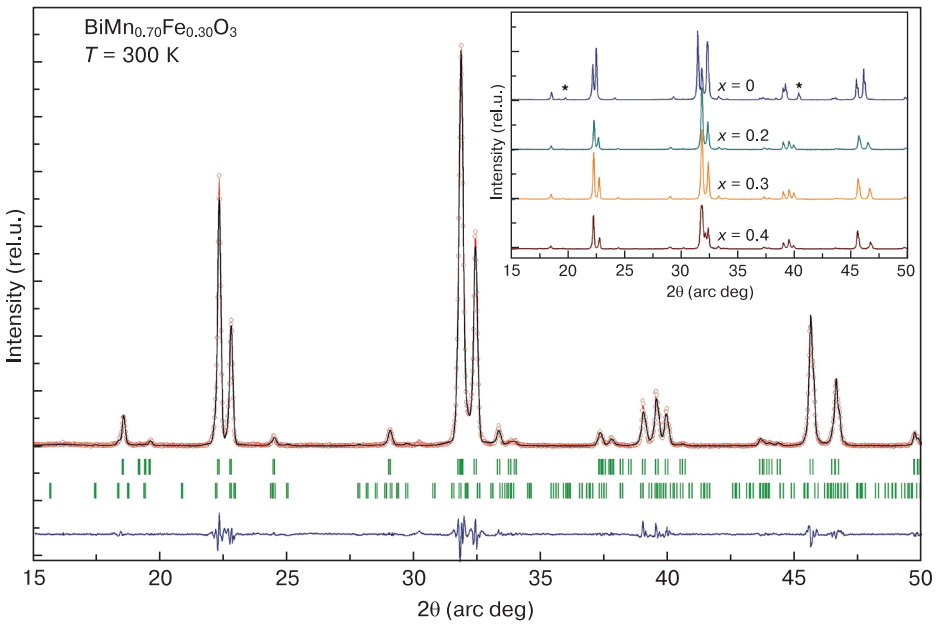

Figure 1. X-ray diffraction pattern of $BiMn_{0.7}Fe_{0.3}O_3$ solid solution corrected in two-phase model: top row of Bragg peaks in a bar diagram form is for monoclinic phase ($C2/c$), bottom row is for orthorhombic phase (*Pnma*). Inset: concentration evolution of reflections typical of two phases in question (the reflections ascribed to the monoclinic phase are marked by the symbol "*")

solution which suggests the presence of two phases, the predominant one remaining the monoclinic phase typical of the $BiMnO_3$ composition and the fraction of the orthorhombic phase being ~20%. It should be noted that the diffraction patterns of the solid solutions with $x > 0$ do not exhibit reflections corresponding to the monoclinic phase (Fig. 1, inset) due to the superimposition of the reflections typical of the two phases in question. Analysis of the X-ray diffraction data showed that further increase in the concentration of iron ions leads to a rapid decrease in the volume fraction of the monoclinic phase and the $BiMn_{0.6}Fe_{0.4}O_3$ composition has an almost single-phase structure with orthorhombic distortions of the unit cell. This concentration phase transition is accompanied by a gradual decrease in the unit cell parameters suggesting the formation of a continuous sequence of solid solutions in the entire test concentration range, which is in agreement with earlier literary data [17, 18].

3.2. Piezoelectric and ferroelectric properties of $BiMn_{1-x}Fe_xO_3$

The initial domain structure of the test specimens features a moderate number of domains from several hundreds of nanometers to 1 mm in diameter inhomogeneously distributed on the specimens surface. The specimens exhibit both vertical and lateral random polarization components. By and large, the number of the domains with predominant random polarization direction in the scanning plane is less than those with polarization in orthogonal planes.

Figure 2 *a–f* shows images of the piezoresponse signal after repolarization with a ±20 V bias for the $BiMn_{1-x}Fe_xO_3$ solid solutions with x = 0.2, 0.3 and 0.4. The polarized areas clearly show the grain boundaries with the grains having a diameter of ~5 mm, and the induced areas replicate the pattern set by the cantilever during DC voltage scanning. There is a piezoresponse signal contrast between the polarized areas. The dark and bright areas suggest opposite polarization vector directions. Analysis of piezoresponse signal phase showed that the dark areas correspond to the domains with the polarization vector directed into the depth of the ceramic surface and the bright ones, to the domains with the polarization vector oriented along the surface. After polarization a series of scans were made showing the evolution of the induced domain structure as a function of time, polarization response signal profiles were plotted and averaging over the middle parts of these images was made (Fig. 2 *d–f*). The induced piezoresponse magnitude decreases with time. Based on the experimental data, the polarization relaxation time was determined to be ~14 min for the $BiMn_{0.7}Fe_{0.3}O_3$ specimen and 7 min for the $BiMn_{0.8}Fe_{0.2}O_3$ specimen. The piezoresponse signal of the $BiMn_{0.6}Fe_{0.4}O_3$ specimen proved to be stable over 1 h of continuous scanning.

In 1 h after polarization and scanning in PFM Kelvin mode, a clear surface potential signal is also observed for the polarized areas in 2 h after polarization (Fig. 3). By analogy with piezoresponse signal images, the surface potential signal maps visualize the grain boundaries.

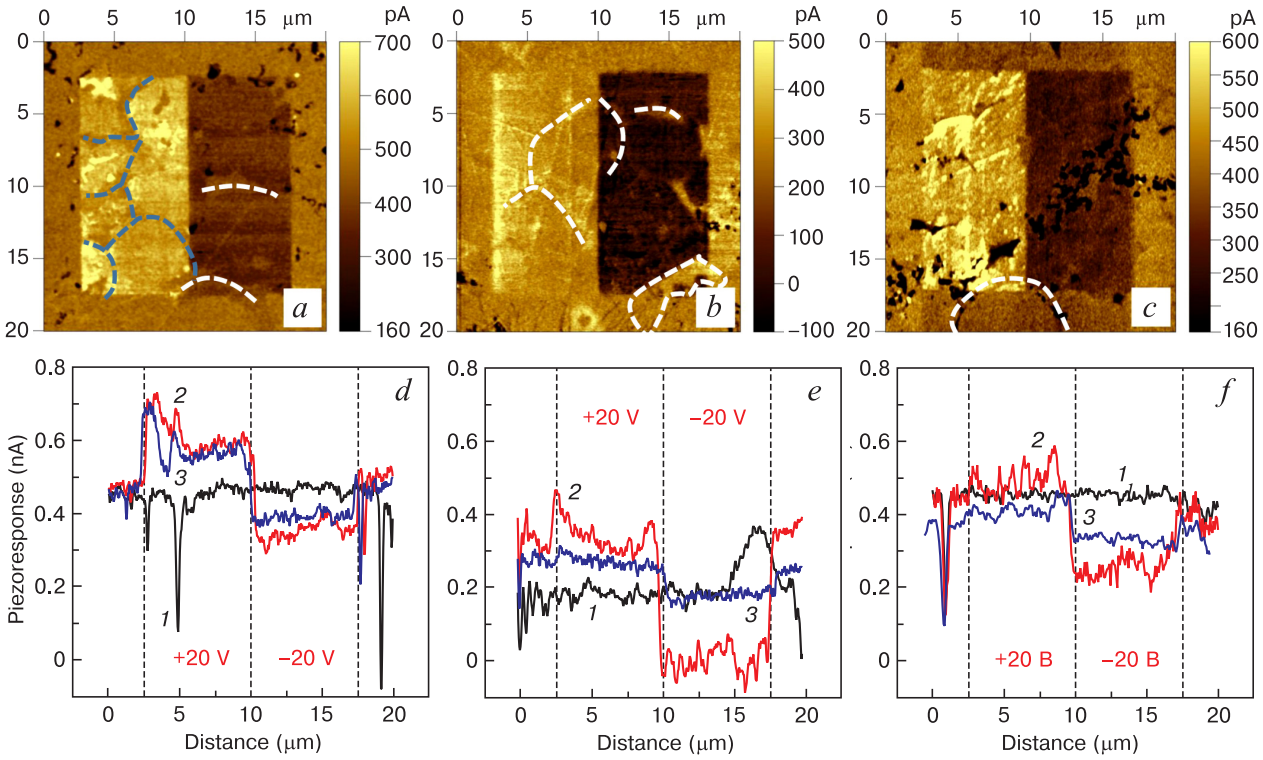

Figure 2. (*a–c*) Piezoresponse signal of $BiMn_{1-x}Fe_xO_3$ solid solutions after polarization with ±20 V bias and (*d–f*) piezoresponse signal profiles for different time after polarization: (*a, c*): x = 0.4; (*b, e*): x = 0.3; (*c, f*): x = 0.2; (*1*) source signal; (*2*) immediately after polarization; (*3*) in 1 h after polarization. Dashes show grain boundaries

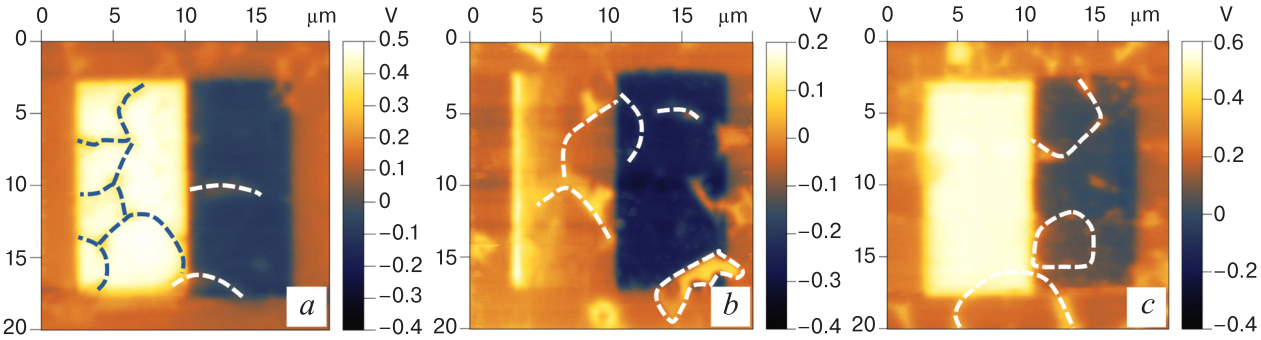

Figure 3. Surface potential signal of $BiMn_{1-x}Fe_xO_3$ solid solutions in 2 h after polarization with ±20 V bias: (*a*) $BiMn_{0.6}Fe_{0.4}O_3$; (*b*) $BiMn_{0.7}Fe_{0.3}O_3$; (*c*) $BiMn_{0.8}Fe_{0.2}O_3$. Dashes show grain boundries

The results suggest that piezoelectric signal decreases dramatically at the grain boundaries in the test specimens and the coercive field magnitude increases, i.e., the 20 V bias used in the experiment proves to be sufficient to change the direction of polarization in the surface layer of grains. Noteworthy, the surface layer of grains typically exhibits a deviation of its chemical composition from the stoichiometric one due to specific features of the synthesis technique. For example, if high-pressure techniques are used, the quantity of oxygen ions decreases (due to oxidation of metallic foils used as specimen containers) resulting in the formation of oxygen vacancies and an increase in the concentration of structural defects in the surface layer which, in turn, shows itself in the observed degradation of the piezoelectric properties.

Residual piezoelectric hysteresis loops were recorded in polarization switching spectroscopy mode (Fig. 4) and also confirm polarization switching on a nanometric scale. The hysteresis loops shown in Fig. 4 are symmetrical and have an internal bias of: –0.6 V for the $BiMn_{0.6}Fe_{0.4}O_3$ composition, +0.17 V for the $BiMn_{0.7}Fe_{0.3}O_3$ composition and +3.67 V for the $BiMn_{0.8}Fe_{0.2}O_3$ composition. By analogy with the polarization of areas (see Fig. 2) the piezoresponse signal at –20 V is greater than at +20 V and is –3.8 and 3.5 pm/V, respectively, for the $BiMn_{0.6}Fe_{0.4}O_3$ composition, –6 and 5.2 pm/V, respectively, for the $BiMn_{0.7}Fe_{0.3}O_3$ composition and ,–2.4 and 1.6 pm/V, respectively, for the $BiMn_{0.8}Fe_{0.2}O_3$ composition.

3.3. Magnetic properties of $BiMn_{1-x}Fe_xO_3$ system solid solutions

The greatest number of magnetic domains and the highest amplitude of their signals were observed for the $BiMn_{0.8}Fe_{0.2}O_3$ composition. The locations of the ferroelectric and magnetic domains are coincident. By way of example, scans of the same regions were taken for the $BiMn_{0,8}Fe_{0,2}O_3$ composition specimen in PFM magnetic mode (Fig. 5).

The magnetic structure of the solid solutions changes dramatically with an increase in the concentration of iron ions due to a change in the structural state of the solid solution. It is well-known that the initial composition $BiMnO_3$ has a ferromagnetic state due to the orbital

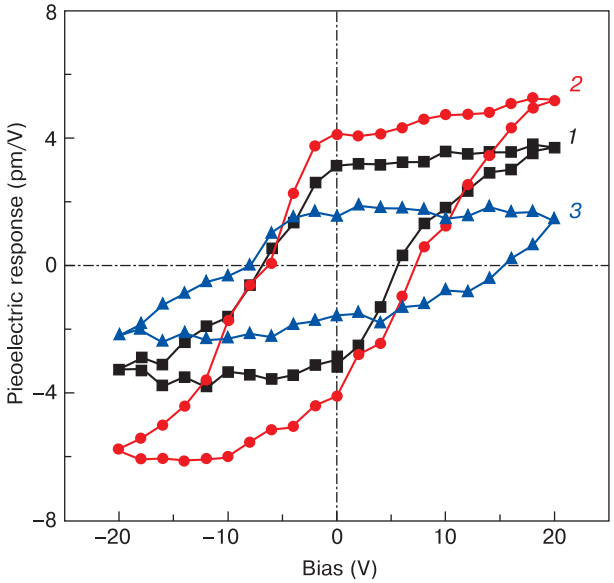

Figure 4. Piezoelectric hysteresis loops of $BiMn_{1-x}Fe_xO_3$ solid solutions: (*1*) $BiMn_{0.6}Fe_{0.4}O_3$; (*2*) $BiMn_{0.7}Fe_{0.3}O_3$; (*3*) $BiMn_{0.8}Fe_{0.2}O_3$

ordering of the Mn^{3+} ions since the $3d^4$ electron configuration of the Mn^{3+} ions causes the Jahn–Teller effect which implies splitting of the e_g energy level (the d_{x2-y2} and d_{z2} orbitals). In this case, the orbital ordering shows itself in that the semi-populated d_{z2} orbital of one Mn^{3+} ion is directed toward the unpopulated d_{x2-y2} orbital of an adjacent Mn^{3+} ion. This produces positive exchange interaction between adjacent manganese ions in accordance with the Goodenough–Kanamori–Andersen theory [22] and leads to the formation of ferromagnetic ordering. The phase transition temperature of the initial $BiMnO_3$ solid solution to the magnetically ordered state is $T_C \sim 100$ K which is in agreement with literary data [13, 18, 23].

Elevated concentration of Fe ions destructs the orbital ordering formed by the ordering of the d_{z2} orbitals of the Mn^{3+} ions and thus leads to the formation of a frustrated magnetic state. Noteworthy, the decrease in the magnetization has a nonlinear pattern. For example, substitution of 20% of manganese ions for iron ions reduces the specific magnetization in a 6 T field from 64.9 to 31.6 emu/g, and for the composition with $x = 0.4$ the magnetization

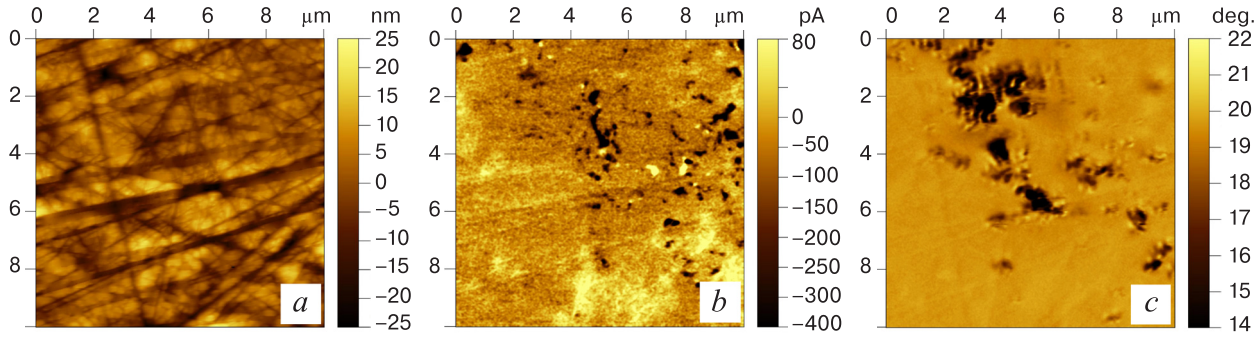

Figure 5. Experimental data for $BiMn_{0.8}Fe_{0.2}O_3$ ceramics: (*a*) topography; (*b*) vertical piezoresponse image; (*c*) magnetic domain structure

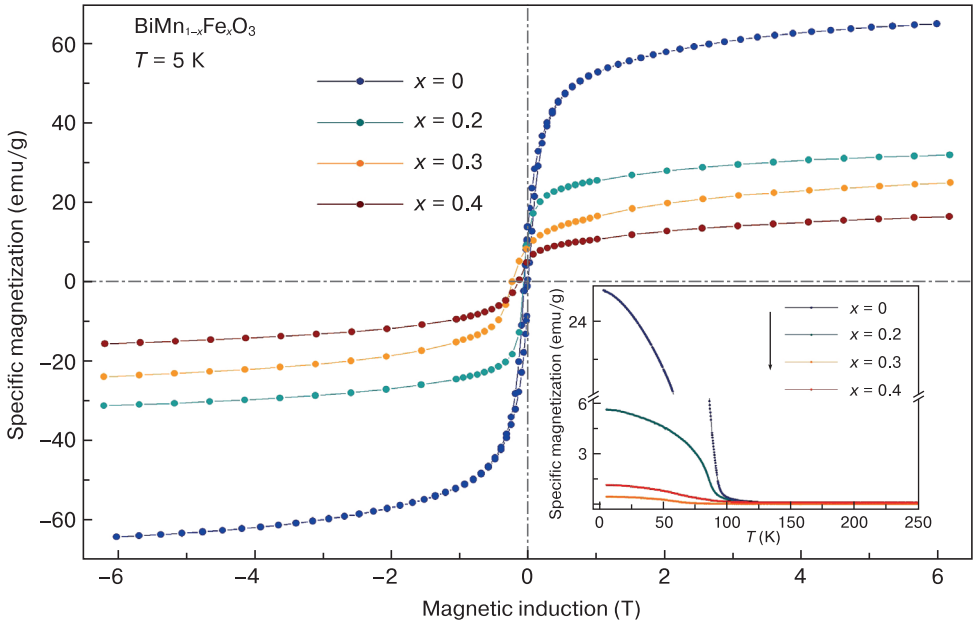

Figure 6. Isothermal magnetization curves for $BiMn_{1-x}Fe_xO_3$ solid solution with $x = 0$, 0.2, 0.3 and 0.4 at $T = 5$ K. Inset: temperature dependence of magnetization taken in cooling mode in a 100 Oe field

is 16.1 emu/g (Fig. 6). The field dependences of magnetization for all the compositions exhibit a clear hysteresis loop at 5 K. The coercive force of the solid solutions with $x = 0$ and 0.2 is less than 0.01 T which is typical of magnetically soft materials while an increase in the concentration of iron ions leads to a significant increase in the coercive force for the compositions with $x = 0.3$ and 0.4 to $H_c = 0.4$ T at 5 K.

The temperature dependences of the magnetization (see Fig. 6, inset) for all the experimental solid solution compositions suggest the presence of a phase transition to a magnetically ordered state at below 100 K. An increase in the concentration of iron ions destructs the long-range ferromagnetic order produced by the orbital ordering of the Mn^{3+} ions [19] which is accompanied by a decrease in the transition temperature to the magnetically ordered state. The composition with $x = 0.4$ exhibits a slight increase in the magnetic transition temperature, probably due to the formation of magnetic ordering in the Fe^{3+} ions. It should be noted that the structural state of the solid solution with $x = 0.4$ features predominantly the orthorhombic phase which implies the absence of orbital ordering in the Mn^{3+} ions, and an additional ferromagnetic component in the magnetic system of these compositions is caused by a noncollinear antiferromagnetic structure formed by the Fe^{3+} ions due to the Dzyaloshinskii–Moriya interaction [24].

4. Conclusion

The structure, piezoelectric and ferroelectric properties of $BiMn_{1-x}Fe_xO_3$ solid solutions ($x \leq 0.4$) were studied. The study showed that an increase in the concentration of substituting ions causes a phase transition from a monoclinic to an orthorhombic structure. The solid solutions with $0.2 \leq x \leq 0.4$ feature non-zero piezoresponse, the polarization switching bias decreasing with an increase in the iron concentration. An increase in the concentration of iron ions in the $BiMn_{1-x}Fe_xO_3$ solid solution system destructs the ferromagnetic state produced by the orbital ordering of the Mn^{3+} ions. The compositions with the predominant orthorhombic phase feature a ferromagnetic component caused by a noncollinear arrangement of the

magnetic moments of the Fe^{3+} ions. Due to the presence of both magnetic and electric dipole ordering these materials show good promise for practical applications in devices based on magnetoelectric interaction.

Acknowledgment

The study was carried out with support of the Russian Science Foundation (21-19-00386).

References

1. Khomskii D. Classifying multiferroics: Mechanisms and effects. *Physics*. 2009; 2: 20. https://doi.org/10.1103/Physics.2.20
2. Scott J.F. Multiferroic memories. *Nature Materials*. 2007; 6(4): 256–257. https://doi.org/10.1038/nmat1868
3. Vaz C.A.F., Hoffman J., Ahn Ch.H., Ramesh R. Magnetoelectric coupling effects in multiferroic complex oxide composite structures. *Advanced Materials*. 2010; 22(26-27): 2900–2918. https://doi.org/10.1002/adma.200904326
4. Yoneda Y., Kitanaka Y., Noguchi Y., Miyayama M. Electronic and local structures of Mn-doped $BiFeO_3$ crystals. *Physical Review B. Condensed Matter*. 2012; 86(18): 184112. https://doi.org/10.1103/PhysRevB.86.184112
5. Kimura T., Goto T., Shintani H., Ishizaka K., Arima T., Tokura Y. Magnetic control of ferroelectric polarization. *Nature*. 2003; 426(6962): 55–58. https://doi.org/10.1038/nature02018
6. Bernardo M.S. Synthesis, microstructure and properties of $BiFeO_3$-based multiferroic materials: A review. *Boletin de la Sociedad Espanola de Ceramica y Vidrio*. 2014; 1(53): 1–14. https://doi.org/10.3989/cyv.12014
7. Neaton J.B., Ederer C., Waghmare U.V., Spaldin N.A., Rabe K.M. First-principles study of spontaneous polarization in multiferroic $BiFeO_3$. *Physical Review B. Condensed Matter*. 2005; 71(1): 14113. https://doi.org/10.1103/PhysRevB.71.014113
8. Catalan G., Scott J.F. Physics and applications of bismuth ferrite. *Advanced Materials*. 2009; 21(24): 2463–2485. https://doi.org/10.1002/adma.200802849
9. Efremov D.V., Van den Brink J., Khomskii D.I. Bond-versus site-centred ordering and possible ferroelectricity in manganites. *Nature Materials*. 2004; 3(12): 853–856. https://doi.org/10.1038/nmat1236
10. Selbach S.M., Tybell T., Einarsrud M.A., Grande T. Structure and properties of multiferroic oxygen hyperstoichiometric $BiFe_{1-x}Mn_xO_{3+\delta}$. *Chemistry of Materials*. 2009; 21(21): 5176–5186. https://doi.org/10.1021/cm9021084
11. Stokes H.T., Kisi E.H., Hatch D.M., Howard Ch.J. Group-theoretical analysis of octahedral tilting in ferroelectric perovskites. *Acta Crystallographica Section B: Structural Science*. 2002; 58(Pt 6): 934–938. https://doi.org/10.1107/S0108768102015756
12. Palai R., Katiyar R.S., Schmid H., Tissot P., Clark S.J., Robertson Jv., Redfern S., Catalan G., Scott J.F. Beta phase and gamma-beta metal-insulator transition in multiferroic $BiFeO_3$. *Physical Review B. Condensed Matter*. 2008; 77(1): 014110. https://doi.org/10.1103/PhysRevB.77.014110
13. Belik A.A. Origin of magnetization reversal and exchange bias phenomena in solid solutions of $BiFeO_3$–$BiMnO_3$: intrinsic or extrinsic? *Inorganic Chemistry*. 2013; 52(4): 2015–2021. https://doi.org/10.1021/ic302384j
14. Denning D., Guyonnet J., Rodriguez B.J. Applications of piezoresponse force microscopy in materials research: from inorganic ferroelectrics to biopiezoelectrics and beyond. *International Materials Reviews*. 2016; 61(1): 46–70. https://doi.org/10.1179/1743280415Y.0000000013
15. Gannepalli A., Yablon D.G., Tsou A.H., Proksch R. Corrigendum: Mapping nanoscale elasticity and dissipation using dual frequency contact resonance AFM. *Nanotechnology*. 2013; 24: 159501. https://doi.org/10.1088/0957-4484/24/15/159501
16. Guennou M., Bouvier P., Chen G.S., Dkhil B., Haumont R., Garbarino G., Kreisel J. Multiple high-pressure phase transitions in $BiFeO_3$. *Physical Review B. Condensed Matter*. 2011; 84(17): 174107. https://doi.org/10.1103/physrevb.84.174107
17. Mumtaz F., Jaffari G.H., Syed S., Khan S. Model-based quantification of inter-intra-grain electrical parameters, hopping polydispersivity, and local energy barrier profile of $BiFeMnO_3$ synthesized by different methods. *Journal of Physics and Chemistry of Solids*. 2022; 160: 110334. https://doi.org/10.1016/j.jpcs.2021.110334
18. Azuma M., Kanda H., Belik A.A., Shimakawa Y., Takano M. Magnetic and structural properties of $BiFe_{1-x}Mn_xO_3$. *Journal of Magnetism and Magnetic Materials*. 2007; 310(2): 1177–1179. https://doi.org/10.1016/j.jmmm.2006.10.287
19. Karpinsky D.V., Silibin M.V., Latushka S.I., Zhaludkevich D.V., Sikolenko V.V., Svetogorov R., Sayyed M.I., Almousa N., Trukhanov A., Trukhanov S., Belik A.A. Temperature-driven transformation of the crystal and magnetic structures of $BiFe_{0.7}Mn_{0.3}O_3$. *Nanomaterials*. 2022; 12(16): 2813. https://doi.org/10.3390/nano12162813
20. Karpinsky D.V., Silibin M.V., Zhaludkevich D.V., Latushka S.I., Sikolenko V.V., Többens D.M., Sheptyakov D., Khomchenko V.A., Belik A.A. Crystal and magnetic structure transitions in $BiMnO_{3+\delta}$ ceramics driven by cation vacancies and temperature. *Materials (Basel)*. 2021; 14(19): 5805. https://doi.org/10.3390/ma14195805
21. Belik A.A. Structural, magnetic, and dielectric properties of solid solutions between $BiMnO_3$ and $YMnO_3$. *Journal of Solid State Chemistry*. 2017; 246: 8–15. https://doi.org/10.1016/j.jssc.2016.10.025
22. Goodenough J.B. Theory of the role of covalence in the perovskite-type manganites [La, *M* (II)] MnO_3. *Physical Review*. 1955; 100(2): 564. https://doi.org/10.1103/PhysRev.100.564
23. Belik A. A. Local distortions in multiferroic $BiMnO_3$ as a function of doping. *Sci. Technol. Adv. Mater.*. 2011; 12(4): 044610. http://dx.doi.org/10.1088/1468-6996/12/4/044610
24. Ederer C., Spaldin N.A. Weak ferromagnetism and magnetoelectric coupling in bismuth ferrite. *Physical Review B. Condensed Matter*. 2005; 71: 060401(R). https://doi.org/10.1103/PhysRevB.71.060401